Applied Catalysis B: Environmental 115–116 (2012) 330–335

Contents lists available at SciVerse ScienceDirect

Applied Catalysis B: Environmental

journal homepage: www.elsevier.com/locate/apcatb

Band structure controls of $SrTiO_3$ towards two-step overall water splitting

Shoichi Hara [a], Hiroshi Irie [b,c,*]

[a] Special Educational Program on Clean Energy, Interdisciplinary Graduate School of Medicine and Engineering, University of Yamanashi, 4-3-11 Takeda, Kofu, Yamanashi 400-8511, Japan
[b] Clean Energy Research Center, University of Yamanashi, 4-3-11 Takeda, Kofu, Yamanashi 400-8511, Japan
[c] Japan Science and Technology Agency, CREST, 5 Sanbancho, Chiyoda-ku, Tokyo 102-0075, Japan

ARTICLE INFO

Article history:
Received 12 October 2011
Received in revised form
25 December 2011
Accepted 28 December 2011
Available online 4 January 2012

Keywords:
Hydrogen
Oxygen
Photocatalysis
Sacrificial agent
Light

ABSTRACT

We prepared two types of $SrTiO_3$-based photocatalyst powders, Bi,Ga-doped $SrTiO_3$ and In,V-doped $SrTiO_3$. UV–visible reflectance spectra of these powders indicated that their band-gaps remained constant in comparison with that of $SrTiO_3$. In conjunction with the reported band structure control of oxides, our results indicated that Bi,Ga-doped $SrTiO_3$ and In,V-doped $SrTiO_3$ formed isolated mini-bands composed of Bi 6s orbitals in the forbidden band above the valence band, composed of O 2p, and V 3d orbitals below the conduction band, composed of Ti 3d, resulting in the observed visible-light absorption. Utilizing the prepared $SrTiO_3$-based photocatalysts, we established a two-step overall water-splitting system, in which simultaneous liberation of hydrogen and oxygen with a molar ratio of ~2:1 was observed in the presence of I^- (NaI) under irradiation with UV-containing light. Moreover, visible light contributed the cycling of I^-/IO_3^- redox mediators, resulting in enhanced hydrogen and oxygen liberation when compared to irradiation with UV light alone.

1. Introduction

Various photocatalytic materials aimed at water splitting have been evaluated because the generated hydrogen (H_2) represents a clean and renewable fuel source [1–4]. Among these materials, $SrTiO_3$ is a promising photocatalyst due to its thermal stability and high resistance against photo-corrosion; however, as $SrTiO_3$ powder alone cannot split water into H_2 and oxygen (O_2), In fact, Yoneyama et al. reported that reduced $SrTiO_3$ powder could decompose water into H_2 and O_2 in stoichiometric amounts [5]. However, the rate of the decomposition showed a tendency to diminish with illumination time (Appendix A). So, in general, the modification is necessary for $SrTiO_3$ to function as an active photocatalyst. NiO modification of $SrTiO_3$ has been found to facilitate the catalytic water-splitting into H_2 and O_2 when irradiated with UV light [6,7]. To further develop the applicability of $SrTiO_3$, improving the visible-light sensitivity of this material is required to effectively utilize incoming solar energy.

To realize the visible-light sensitivity of $SrTiO_3$, numerous studies have examined the doping of foreign elements into the lattice of $SrTiO_3$. Doped $SrTiO_3$ is able to generate either H_2 or O_2 in the presence of sacrificial agents following irradiation with visible light (half water-splitting) [8]. Combined systems consisting of doped $SrTiO_3$ and a second photocatalyst, such as Pt-deposited Cr,Ta-doped $SrTiO_3$ or Rh-doped $SrTiO_3$ serving as the H_2-production photocatalyst, and Pt-deposited WO_3 or $BiVO_4$ as the O_2-production photocatalyst, can function as visible-light sensitive photocatalysts for overall water-splitting in the presence of a suitable redox couple (two-step overall water-splitting) [9–11]. Very recently, Maeda et al. successfully created such a system using only TaON-based photocatalysts [12]. In the present study, we have established a two-step overall water-splitting system by combining only $SrTiO_3$-based materials. To our knowledge, this is the first study to generate a photocatalyst system by introducing foreign elements into the identical mother structure, whose electronic band structure was controlled.

2. Experimental

2.1. Preparation of $SrTiO_3$-based photocatalysts

$SrTiO_3$ (STO) was synthesized using a conventional solid-state reaction. Commercial $SrCO_3$ (Kanto Kagaku) and TiO_2 (High Purity Chemicals) powders were used as the starting materials. Stoichiometric amounts of the starting materials were wet-ball milled for 20 h using ZrO_2 balls as the milling medium in polyethylene bottles. The resulting mixture was calcined at 1100 °C for 6 h and then thoroughly ground. $(Bi_{0.1}Sr_{0.9})(Ti_{0.9}Ga_{0.1})O_3$ (Bi,Ga-STO) was also

* Corresponding author at: Clean Energy Research Center, University of Yamanashi, 4-3-11 Takeda, Kofu, Yamanashi 400-8511, Japan. Tel.: +81 55 220 8092; fax: +81 55 220 8092.
E-mail address: hirie@yamanashi.ac.jp (H. Irie).

0926-3373/$ – see front matter © 2012 Elsevier B.V. All rights reserved.
doi:10.1016/j.apcatb.2011.12.042

synthesized by the solid-state reaction using prepared STO, commercially available Bi_2O_3 (Kanto Kagaku), and Ga_2O_3 (Wako) as the starting materials. The starting materials were wet ball-milled for 20 h in ratios corresponding to the composition of Bi,Ga-STO. The powders were heated at 750 °C for 6 h. The obtained powders were pressed into pellets, heated at 1100 °C for 6 h, and then thoroughly ground. $Sr(V_{0.005}Ti_{0.99}In_{0.005})O_3$ (In,V-STO) and $Sr(In_{0.03}Ti_{0.94}V_{0.03})O_3$ (In,V-STO2) were also synthesized by the solid-state reaction. In,V-STO was synthesized using prepared STO, commercially available $SrCO_3$, In_2O_3 (Wako), and V_2O_5 (Kanto Kagaku) and In,V-STO2 was using commercially available $SrCO_3$, TiO_2, In_2O_3, and V_2O_5 as the starting materials. Those starting materials were wet-ball milled for 20 h in ratios corresponding to the compositions of In,V-STO and In,V-STO2. The obtained powders for In,V-STO and In,V-STO2 were heated at 600 and 1100 °C, respectively, for 6 h, and then thoroughly ground.

The deposition of Pt co-catalyst onto STO, Bi,Ga-STO and In,V-STO2 was performed by a photo-decomposition method [13]. Briefly, 0.5 g of either STO, Bi,Ga-STO or In,V-STO2 powder was first dispersed in 80 mL distilled water containing 20 mL methanol. H_2PtCl_6, acting as the source of Pt, was then weighed to give a weight fraction of Pt relative to either STO, Bi,Ga-STO or In,V-STO2 of 1×10^{-3}. The weighed H_2PtCl_6 was added to the aqueous sample suspension, which was then sufficiently deaerated using liquid N_2. While deaerating, a Xe lamp (LA-251Xe; Hayashi Tokei) was employed for light irradiation of the suspension for 4 h. The suspension was then filtered with a membrane filter (5–10 μm; Whatman) and washed with sufficient amounts of distilled water. The resulting residues were dried at 80 °C for 24 h and then ground into a fine powder using an agate mortar.

2.2. Characterizations

The crystal structures of the prepared powders were examined by X-ray diffraction (XRD) using a PW-1700 system (Panalytical). UV–visible absorption spectra were obtained by the diffuse reflection method using UV-2550 (Shimadzu) and V-650 (JASCO) spectrometers.

2.3. Photocatalytic water-splitting tests

The following two types of photocatalytic water-splitting tests were performed in a gas-closed-circulation system that was filled with argon gas (50 kPa), which was introduced into the system after deaeration. The amounts of evolved H_2 and O_2 were monitored using an online gas chromatograph (GC-8A; Shimadzu).

(1) Pt/Bi,Ga-STO and In,V-STO mixed powder (30 mg each) and Pt/Bi,Ga-STO and Pt/In,V-STO2 mixed powder (48 and 12 mg, respectively) with I^- (NaI; Kanto Kagaku, 0.01 mol/L) as a redox mediator was suspended in 10 mL water at pH 7 using a magnetic stirrer. A Xe lamp without a glass filter was employed for light irradiation. The reaction was allowed to proceed repeatedly with evacuation every 48 h after pre-irradiation for a proper period to stabilize the water-splitting reaction. In the present study, the reaction temperature was neither controlled nor monitored. In this case we additionally performed the reaction under irradiated light from Xe lamp filtered through water to remove infrared photons and under cooling condition with water (Appendix B). For comparison, the identical test using Pt/STO powder (60 mg) in place of the mixtures of Pt/Bi,Ga-STO and either In,V-STO or Pt/In,V-STO2 was performed. In addition, the water-splitting test using Pt/STO powder (60 mg) in distilled water (pH 7) without added redox mediators was also performed under Xe-lamp irradiation.

(2) Pt/Bi,Ga-STO and In,V-STO mixed powder (30 mg each) with I^- (NaI; 0.01 mol/L) as the redox mediator was suspended in 10 mL water at pH 7 using a magnetic stirrer. A Xe lamp equipped with either a single (U340; Hoya) or two glass filters (L42 and B410; Hoya) was employed for UV-light irradiation with wavelengths of 300–400 nm and visible-light irradiation with wavelengths of 400–600 nm, respectively. In addition, the simultaneous irradiation with these UV and visible lights were performed.

3. Results and discussion

3.1. Characterization of $SrTiO_3$-based photocatalysts

The XRD patterns of the synthesized STO, Bi,Ga-STO, In,V-STO and In,V-STO2 powders indicated a cubic crystal structure with a perovskite crystalline phase (Fig. 1a). STO, Bi,Ga-STO and In,V-STO were confirmed to have a single phase of cubic STO, whereas a small amount of impurity was detected in In,V-STO2. In Fig. 1b, the peaks of In,V-STO and In,V-STO2 shifted to lower 2θ angle, compared to non-doped STO. That of In,V-STO2 was largely shifted, compared to In,V-STO. These are reasonable when we consider the effective ionic radii of Ti^{4+}, In^{3+} and V^{5+} (six-coordination) are 0.061, 0.079 and 0.054 nm, respectively. In addition, the effective ionic radius of Sr^{2+} (twelve-coordination) is 0.144 nm, which is much larger than those of Ti^{4+}, In^{3+} and V^{5+}. Even when comparing the ionic radii with the same coordination number, that of Sr^{2+} (six-coordination) is 0.116 nm, being much bigger than those of Ti^{4+}, In^{3+} and V^{5+}. So, it is unlikely that Sr sites were replaced by In and V ions. Thus, we could confidently conclude that In and V ions were incorporated at Ti sites in In,V-STO and In,V-STO2. Note that *A* and *B* sites in the ABO_3 perovskite structure are twelve- and six-coordinated, respectively.

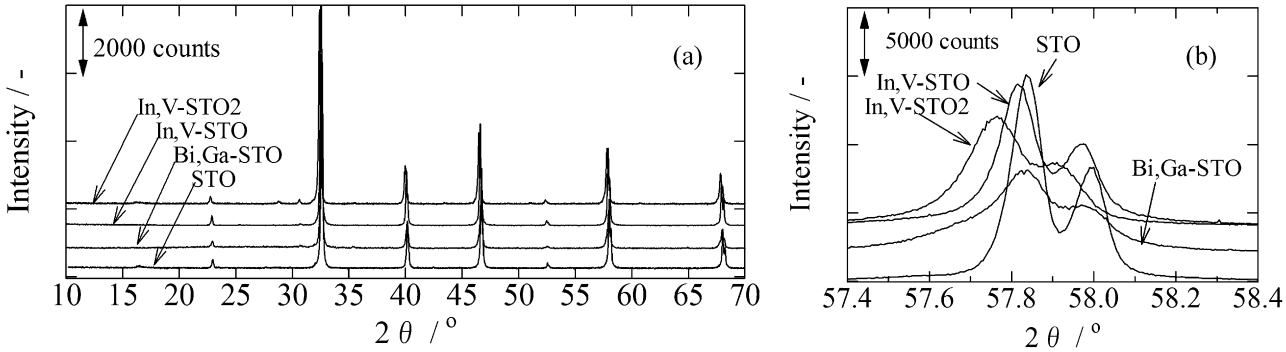

Fig. 1. XRD patterns of prepared STO, Bi,Ga-STO, In,V-STO and In,V-STO2 powders. The XRD patterns in (b) were obtained by the precise measurements with a step length of 0.005° and a step-counting time of 4 s.

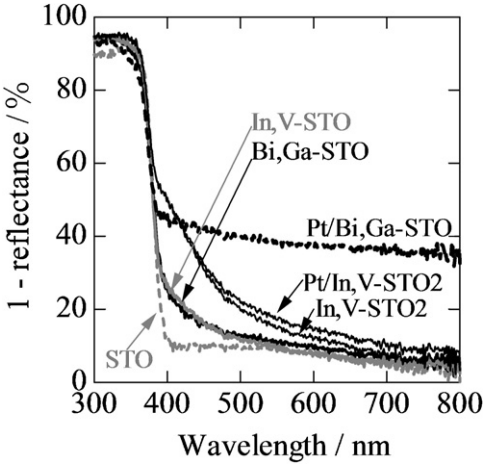

Fig. 2. UV–visible absorption spectra of STO, Bi,Ga-STO, In,V-STO, In,V-STO2, Pt/Bi,Ga-STO, and Pt/In,V-STO2. For Bi,Ga-STO and In,V-STO, nearly identical absorption shoulders in the visible-light region up to ~520 nm were observed. After Pt deposition onto Bi,Ga-STO and In,V-STO2, increased absorption at a wider wavelength region (>400 nm) in each photocatalyst was observed.

The effective ionic radius of Bi^{3+} (twelve-coordination) is unknown, so here, we adopt the one of Bi^{3+} (six-coordination) of 0.102 nm. That of Bi^{3+} (six-coordination) is smaller than that of Sr^{2+} (six-coordination, 0.116 nm), whereas that of Ga^{3+} (six-coordination, 0.062 nm) is slightly larger than that of Ti^{4+} (six-coordination, 0.061 nm). Thus, the peak of Bi,Ga-STO was expected to shift to higher 2θ angle, compared to STO, however, it was unchanged as shown in Fig. 1b. It is presumably plausible as follows; the crystallinity of Bi,Ga-STO was quite lower than that of STO, considering from the lower intensity and broader peak. It is reasonable that Bi and Ga were introduced as "impurities". Then, it might be possible that the lattice constant of Bi,Ga-STO is larger than that of STO. This causes the lower shift of 2θ angle, and thus the peak shift cancelled out. Although 2θ angle of the peak was unchanged after introducing Bi and Ga into STO, the ionic radius of Bi^{3+} is too large to replace at the Ti^{4+} site, and that of Ga^{3+} is too small to replace at the Sr^{2+} site. So, we concluded that Bi and Ga ions were incorporated at Sr and Ti sites in Bi,Ga-STO, respectively.

In Fig. 2, the UV–visible absorption spectra of STO, Bi,Ga-STO, In,V-STO, In,V-STO2, Pt-deposited Bi,Ga-STO (Pt/Bi,Ga-STO) and Pt-deposited In,V-STO2 (Pt/In,V-STO2) are shown. For Bi,Ga-STO, In,V-STO and In,V-STO2, the formation of absorption shoulders in the visible-light region and negligible shifts of the absorption edges were observed. These findings indicate that the band-gaps in both materials did not narrow, although isolated mini-bands formed in the forbidden band.

For comparison, $(La_{0.2}Sr_{0.8})(Ti_{0.8}Ga_{0.2})O_3$ (La,Ga-STO), $Sr(In_{0.02}Ti_{0.96}Ta_{0.02})O_3$ (In,Ta-STO) and $(Na_{0.01}Sr_{0.99})(Ti_{0.99}V_{0.01})O_3$ (Na,V-STO) powders were prepared and evaluated. For La,Ga-STO and In,Ta-STO, the spectra were unchanged compared to STO. In contrast, visible-light absorption was generated for Na,V-STO, identical to Bi,Ga-STO, In,V-STO and In,V-STO2 (Appendix B). These findings clearly indicated that both Bi and V ions were responsible for the visible-light absorption capability in Bi,Ga-STO and In,V-STO, respectively.

Numerous reports have examined the band structure control of oxides towards increasing sensitivity to visible light [14–16]. Some of these studies have revealed that Bi 6s orbitals are energetically comparable to O 2p or higher [15], which compose the valence band (VB), while V 3d orbitals are energetically lower than Ti 3d [16], which form the conduction band (CB). Thus, we confidently concluded that Bi,Ga-STO formed isolated mini-bands composed of Bi 6s orbitals in the forbidden band above the VB composed of O 2p, and that In,V-STO and In,V-STO2 formed isolated mini-bands composed of V 3d orbitals in the forbidden band below the CB composed of Ti 3d, resulting in the observed visible-light absorption. It is probable that oxygen vacancy generated to some extent by doping foreign elements. According to the previous reports [17], the oxygen vacancy state is below the lower end of the CB at 0.75–1.18 eV and thus, the STO with oxygen vacancies can absorb a broad range of visible light above 500 nm. As shown in Fig. 2, the absorptions of Bi,Ga-STO and In,V-STO above 500 nm were quite similar to that of non-doped STO. In the case of In,V-STO2, the absorption above 500 nm originated from V 3d was so large that the one from oxygen vacancies was masked. So, in the present study, we considered that the effect of oxygen vacancies generated by introducing dopants could be negligible. Pt was successfully deposited onto Bi,Ga-STO and In,V-STO2 powders, as the absorption at a wider wavelength region (>400 nm) increased. The increase in Pt/Bi,Ga-STO was much larger than that in Pt/In,V-STO2. In the present study, Pt was deposited under Xe light irradiation in deaerated condition in the presence of H_2PtCl_6 [13]. Then Pt^{4+} was reduced to Pt by photo-excited electrons in the CB in the case of

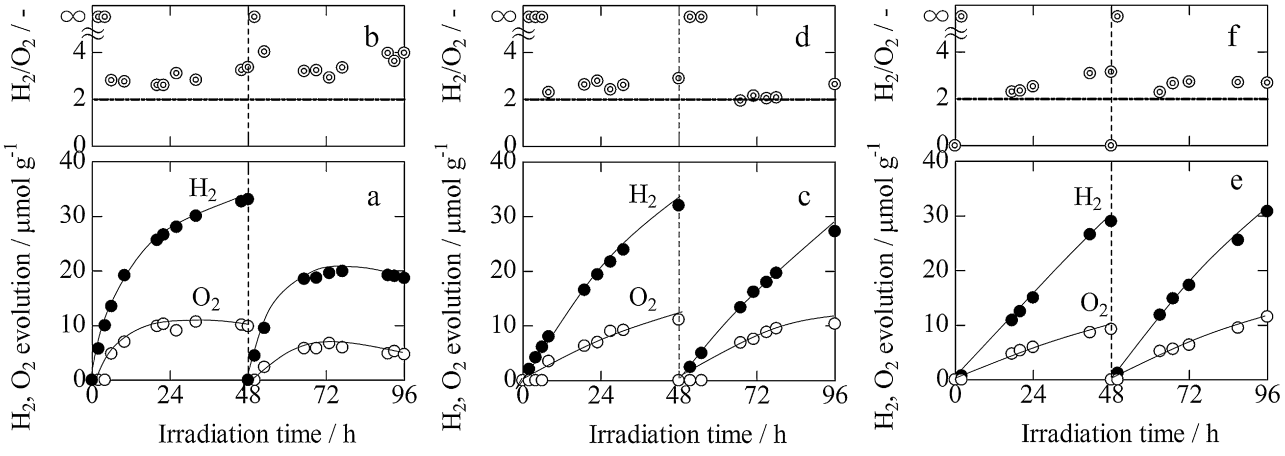

Fig. 3. Time courses of H_2 (closed circles) and O_2 (open circles) evolution by water-splitting as a function of time in the presence of (a) Pt/STO, (c) Pt/Bi,Ga-STO and In,V-STO, and (e) Pt/Bi,Ga-STO and Pt/In,V-STO2 photocatalysts irradiated with a Xe lamp. The reaction was allowed to proceed for 98 h with evacuation every 48 h. (b), (d) and (f) show the ratio of evolved H_2 to O_2 obtained from the data in (a), (c) and (e), respectively. When O_2 evolution was not detected, but H_2 was detected in the initial period of the cycle, the ratio was indicated as ∞. In (d) and (f), the H_2/O_2 ratio is nearly two, indicating that complete water-splitting was accomplished; however, in (b), the ratio increasingly deviated from the stoichiometric ratio of two with increasing number of evacuation cycles.

Bi,Ga-STO, whereas by those both in the CB and in the V 3d miniband in the case of In,V-STO2. The photo-excited electrons in the CB diffuse to the surface through Ti 3d orbital to reduce Pt^{4+} to Pt. So, it might be probable that the dopant V ions as "impurities" at Ti site prevent photo-excited electrons from diffusion to the surface. Moreover, the reduction power of electrons in the V 3d state is smaller than those in the CB. In contrast, Ti 3d orbital was scarcely affected by Bi and Ga ions. Thus it is reasonable that the amount of deposited Pt was larger on the surface of Bi,Ga-STO, resulting in the larger increase in the wider wavelength region.

3.2. Photocatalytic water-splitting tests

We examined water-splitting by Pt/STO, utilizing I^- as a sacrificial agent, under irradiation with a Xe lamp for 96 h, with evacuation of the system every 48 h (Fig. 3a and b). Although the evolution of both H_2 and O_2 was initially observed in each 48 h cycle, their evolution decreased and eventually ceased with increasing irradiation time in each cycle. In addition, the irradiation time when H_2 and O_2 levels started to decrease occurred more rapidly following each subsequent evacuation. This finding is plausible because the existence of I^- served as the sacrificial agent for H_2 evolution, which was initiated by the photo-excited electrons in the CB of STO. In contrast, the holes in the VB of STO competitively oxidized I^- and H_2O to produce IO_3^- and O_2, respectively ($E^0(IO_3^-/I^-) = 0.67$ V vs. SHE, pH 7) [18]. For this reason, the amount of IO_3^- formed as a result of I^- oxidation would be expected to increase with increasing irradiation time, resulting in the use of photo-excited electrons to reduce IO_3^- instead of H_2O. Thus, in this system, photo-excited electrons and holes were consumed to reduce IO_3^- and oxidize I^-, respectively, resulting in the cessation of H_2 and O_2 evolution. Because the evacuation was performed prior to the next cycle, the generated IO_3^- might be reduced to I^-. This would be expected to re-initiate H_2 and O_2 evolution, however, the evolution of both gases eventually stopped with continued irradiation, similar to the first cycle. The ratio of evolved H_2 to O_2 for

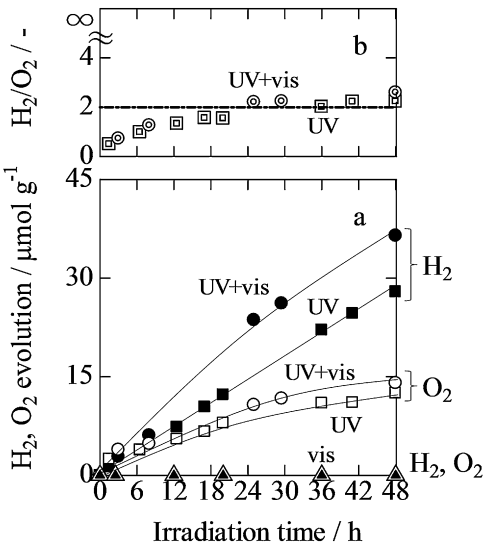

Fig. 4. (a) Time courses of H_2 (closed marks) and O_2 (open marks) evolution by water-splitting as a function of time in the presence of both Pt/Bi,Ga-STO and In,V-STO under irradiation with only UV light (squares), only visible light (triangles), and a combination of UV and visible light (circles) in the presence I^-. (b) Ratio of evolved H_2 to O_2 obtained from the data in (a). In (b), the H_2/O_2 ratio was approximately two when the system was irradiated with UV light and a combination of UV and visible light, indicating that complete water-splitting was accomplished.

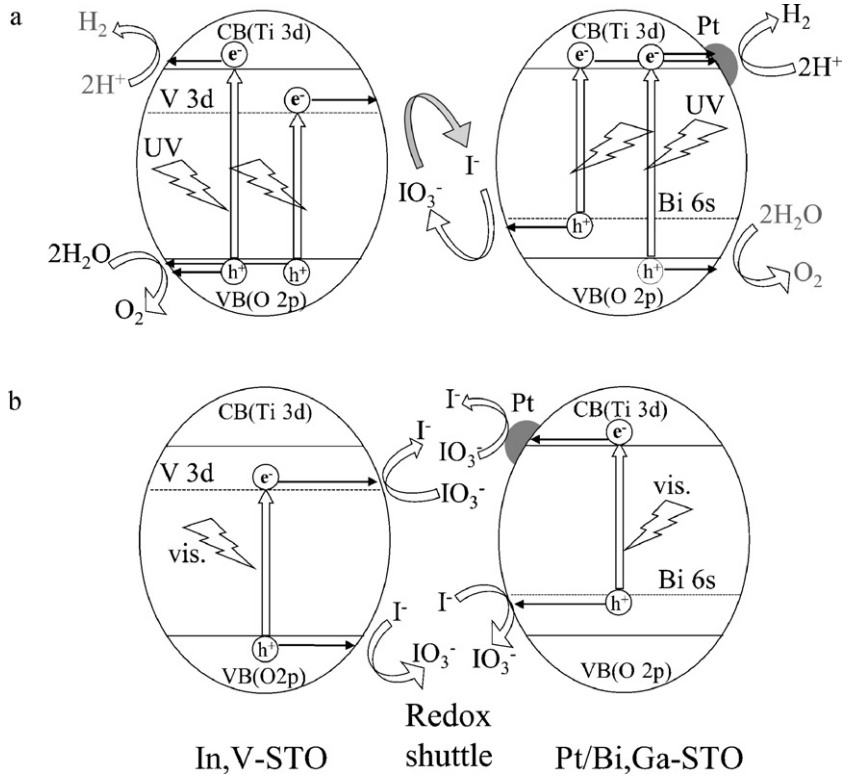

Fig. 5. (a) Schematic illustrations of spontaneous H_2 and O_2 evolution in the presence of In,V-STO and Pt/Bi,Ga-STO with the aid of IO_3^-/I^- redox shuttle under irradiation with UV light. Photo-generated electrons in the CBs of both materials might competitively reduce H_2O to H_2 and IO_3^- to I^-, and photo-generated holes in the VBs might competitively oxidize H_2O to O_2 and I^- to IO_3^-. (b) Schematic illustrations of inactive H_2 and O_2 evolution in the presence of In,V-STO and Pt/Bi,Ga-STO under irradiation with visible light. Neither photo-generated electrons in the CB of Pt/Bi,Ga-STO nor holes in the VB of In,V-STO contribute to the water-splitting reaction. The reaction mechanism in the case of Pt/In,V-STO2 is essentially identical to the case of In,V-STO.

the Pt/STO system increasingly deviated from the stoichiometric ratio of two with increasing number of evacuation cycles (Fig. 3b). Notably, Pt/STO could only generate H_2, but not O_2, in the absence of I^- (in pure distilled water, pH 7) irradiated with the Xe lamp, similar to the case of Ni-modified STO [6].

We next examined the simultaneous evolution of H_2 and O_2 in the presence of both Pt/Bi,Ga-STO and In,V-STO, utilizing I-as the sacrificial agent, under Xe-lamp irradiation (Fig. 3c and d). Again, the reaction was allowed to proceed for 96 h with evacuation every 48 h. In Fig. 3c and d, identical amounts of Pt/Bi,Ga-STO (30 mg) and In,V-STO (30 mg) were used as photocatalysts because the light-absorption capability in the visible-light region (>400 nm) of Bi,Ga-STO and In,V-STO was identical (Fig. 2). In these materials, we controlled the dopant concentrations (Bi^{3+} and V^{5+}) to yield Bi,Ga-STO and In,V-STO with nearly identical visible-light absorption capabilities, because the water-splitting was assumed to be a two-photon reaction system. The ratio of evolved H_2 to O_2 was ~2 to 1 (stoichiometric amount) in every cycle, as shown in Fig. 3d. The ratio of evolved H_2 to O_2 was ~2 to 1 was also observed under irradiated light filtered through water to remove infrared photons and cooling condition with water (Appendix B). In addition, we performed the water-splitting test utilizing Pt/InV-STO2 in place of In,V-STO, in this case, 48 mg of Pt/Bi,Ga-STO and 12 mg of Pt/In,V-STO2 were used as photocatalysts because the light-absorption capability in the visible-light region (>400 nm) of In,V-STO2 was ~4-fold larger than that of Bi,Ga-STO. This system could also simultaneously evolve H_2 and O_2 at a molar ratio of ~2 to 1 (Fig. 3e and f). Thus, overall water-splitting in the system combining two kinds of $SrTiO_3$-based photocatalysts was achieved. It seems that the presence or absence of Pt cocatalyst onto O_2-evolution photocatalyst (In,V-STO, In,V-STO2) did not affect the water-splitting reaction although we should investigate it further. Again note that the H_2 to O_2 ratio in the presence of only Pt/STO deviated from two with increasing number of evacuation cycles.

On consideration of the present experimental results, the steady H_2 and O_2 evolution at a ratio of ~2 to 1 in the presence of Pt/Bi,Ga-STO and either In,V-STO or In,V-STO2 under Xe-lamp irradiation was predominantly attributed to the introduced Bi 6s and V 3d states in the forbidden band of STO. To confirm this speculation, we performed water-splitting in the presence of both Pt/Bi,Ga-STO and In,V-STO, utilizing I^- as the redox mediator, under irradiation with either UV light, visible light, or a combination of UV and visible light, as shown in Fig. 4. The simultaneous evolution of H_2 and O_2 was observed in the system irradiated with only UV light, whereas neither gas was observed on visible-light irradiation. This finding clearly indicates that UV light-excited electrons in the CBs of Bi,Ga-STO and In,V-STO reduce H_2O and produce H_2, and competitively turn-over IO_3^- to I^-, and that UV light-excited holes in the VBs of these materials oxidize H_2O and produce O_2, and competitively turn-over I^- to IO_3^-. Following irradiation with UV light, photoexcitation from the VB of In,V-STO to the V 3d state and from the Bi 6s state to the CB of Bi,Ga-STO also proceeds. Thus, it is probable that photo-excited electrons in the V 3d state and holes in the Bi 6s state contribute to the turn-over of IO_3^- to I^-, and vice versa. Notably, the evolution of H_2 and O_2 under both UV and visible light was greater than that observed under only UV light, suggesting that visible light induces electrons and holes in the V 3d and Bi 6s states, respectively, which contribute to the cycling of IO_3^-/I^-. A possible mechanism for complete water-splitting in the Pt/Bi,Ga-STO and In,V-STO system, as described above, is shown in Fig. 5. Presently, this system needs UV light, however, we believe that the novel method to achieve overall water-splitting utilizing the identical mother structure would provide us with good insight to design photocatalysts for converting solar energy to H_2 energy.

4. Conclusions

We have established a two-step overall water-splitting system utilizing two types of STO-based photocatalysts that simultaneously evolve H_2 and O_2 at a molar ratio of ~2 to 1 in the presence of sacrificial agent following irradiation with light. Presently, this system requires UV light; however, in principle, it should function when irradiated with only visible light. To achieve this property, we are currently applying a hydrothermal method to prepare highly crystallized nano-particulate STO-based photocatalysts and are determining suitable dopant concentrations and co-catalysts. Moreover, as the band-gap and band structure of STO are identical to those of TiO_2, it may be possible to construct the two-step overall water-splitting system utilizing TiO_2-based photocatalysts with the same strategy. This may be advantageous because TiO_2-based photocatalysts are nontoxic, stable, and naturally abundant, which is expected to facilitate their use in industrial and practical applications. Such investigations are currently being conducted in our laboratory.

Acknowledgment

We express gratitude to Mr. G. Newton for the careful reading of the manuscript.

Appendix A.

There are, in fact, some papers that show $SrTiO_3$ (STO) can split water into H_2 and O_2, e.g., M.S. Wrighton et al., J. Am. Chem. Soc., 98 (1976) 2774–2779. Almost of them are the studies in the photoelectrode system using STO and Pt electrodes with or without an applied external potential. However, the system needs the Pt electrode as H_2 evolution site, as well as the STO photoelectrode as O_2 evolution site. So, the photoelectrode system does not work in the presence of STO alone. As far as the reviewer knows, Ref. [5] in the main text reported by Yoneyama et al. is the only study that successfully evolved H_2 and O_2 under illumination in the presence of only STO powder. However, the STO powder in Ref. [5] was reduced by H_2 at 900 °C for 3 h. Although Yoneyama et al. did not characterize the reduced STO, we can easily speculate that such reduced STO contains lots of oxygen vacancies, denoted by $SrTiO_{3-x}$ with a quite large x value. Otherwise STO might be partially decomposed to, such as, SrO_{1-y} and TiO_{2-z}. Moreover, such reduced STO clearly indicated that the rates of H_2 and O_2 evolutions had a tendency to diminish with illumination time. They speculated the reason and attributed it to some change in the surface condition of the catalyst.

Appendix B. Supplementary data

Supplementary data associated with this article can be found, in the online version, at doi:10.1016/j.apcatb.2011.12.042.

References

[1] A. Fujishima, K. Honda, Nature 238 (1972) 37–38.
[2] J. Sato, N. Saito, H. Nishiyama, Y. Inoue, J. Phys. Chem. B 105 (2001) 6061–6063.
[3] H. Kato, K. Asakusa, A. Kudo, J. Am. Chem. Soc. 125 (2003) 3082–3089.
[4] K. Maeda, K. Teramura, D. Lu, T. Takata, N. Saito, Y. Inoue, K. Domen, Nature 440 (2006) 295.
[5] H. Yoneyama, M. Koizumi, H. Tamura, Bull. Chem. Soc. Jpn. 52 (1979) 3449–3450.
[6] K. Domen, A. Kudo, T. Onishi, N. Kosugi, H. Kuroda, J. Phys. Chem. 90 (1986) 292–295.
[7] K. Domen, J.N. Kondo, M. Hara, T. Takata, Bull. Chem. Soc. Jpn. 73 (2000) 1307–1331.
[8] H. Kato, A. Kudo, J. Phys. Chem. B 106 (2002) 5029–5034.
[9] K. Sayama, K. Mukasa, R. Abe, Y. Abe, H. Arakjawa, J. Photochem. Photobiol. A: Chem. 148 (2002) 71–77.
[10] H. Kato, Y. Sasaki, A. Iwase, A. Kudo, Bull. Chem. Soc. Jpn. 80 (2007) 2457–2464.

[11] A. Kudo, Int. J. Hydrogen Energy 32 (2007) 2673–2678.
[12] K. Maeda, R. Abe, K. Domen, J. Phys. Chem. Lett. 115 (2011) 3057–3064.
[13] S. Tabata, H. Nishida, Y. Masaki, K. Tabata, Catal. Lett. 34 (1995) 245–249.
[14] H. Irie, Y. Maruyama, K. Hashimoto, J. Phys. Chem. B 111 (2007) 1847–1852.
[15] J.W. Tang, Z.G. Zou, J. Ye, Angew. Chem. Int. Ed. 43 (2004) 4463–4466.
[16] H. Irie, K. Hashimoto, J. Am. Ceram. Soc. 88 (2005) 3137–3142.
[17] M. Miyauchi, M. Takashiro, H. Tobimatsu, Langmuir 20 (2004) 232–236.
[18] A.J. Bard, R. Parsons, J. Jordan (Eds.), Standard Potentials in Aqueous Solution, Marcel Dekker, New York, U.S.A., 1985.